Crystallization of NiCo MOF-74 on a Porous NiO Film as an Anode for the Urea/H_2O_2 Fuel Cell

Yulia M. T. A. Putri,[1] Thomas W. Chamberlain,[2,3] Volkan Degirmenci,[3] Jarnuzi Gunlazuardi,[1] Yuni K. Krisnandi,[1] Richard I. Walton,[2] and Tribidasari A. Ivandini[1*]*

[1]Department of Chemistry, Faculty of Mathematics and Natural Sciences, Universitas Indonesia, Kampus UI Depok, Jakarta 16-424, Indonesia

[2]Department of Chemistry, University of Warwick, CV4 7AL, Coventry, UK

[3]School of Engineering, University of Warwick, CV4 7AL, Coventry, UK

KEYWORDS: Nickel-Cobalt, porous Nickel Oxide (NiO), MOF-74, Urea Oxidation, Fuel Cell

ABSTRACT. NiCo-MOF-74 crystallized directly on the surface of porous NiO (p-NiO) film using a solvothermal method is proposed as an effective electrocatalyst for the anode in direct urea fuel cells. A nickel-to-cobalt ratio of 4:1 was found to show optimum catalytic activity towards urea oxidation with significant current enhancement in comparison to other electrodes, including Ni foil and p-NiO. At optimized conditions in an electrolyte solution of 3.0 M KOH and 1.0 M urea, a current density of around 110 mA cm^{-2} with a maximum power density of 4131 μW cm^{-2} can be produced. This is ascribed to the increase of the active surface area over conventional nickel-based anodes, providing an abundance of active sites for urea oxidation. Excellent stability and

reproducibility over 15 hours application in a direct urea fuel cell was obtained with cell voltage of ~0.6 V. Powder X-ray diffraction shows the crystalline MOF film remain intact after chronoamperometry tests, and after fuel cell application, illustrating applicability in real devices.

INTRODUCTION: Urea has been widely proposed as an alternative source of fuel as it is non-toxic, has a high reaction efficiency, is easily stored, and inexpensive.[1,2] Urea has a high hydrogen content, around 6.67% by weight with an energy density of 16.9 MJ L^{-1} (ten times greater than hydrogen). In addition, the high abundance of urea makes it a high potential candidate to replace hydrogen as fuel in fuel cells.[3–5] Urea can be found in large quantities in factory waste and from adult humans, who generally excrete 1.5 L of urine containing around 2-2.5% by weight of urea, equivalent to around 11 kg of urea per year.[6–8] However, one major limitation of the urea oxidation reaction (UOR) is slow reaction kinetics. Accordingly, it is necessary to develop a highly efficient UOR electrocatalyst to reduce the reaction limitations and increase the reaction rate.[9–11]

Nickel-based electrodes have been widely known as excellent anode catalysts for UOR in direct urea fuel cells (DUFCs).[12] However, nickel-based catalysts have high formation potentials due to their low conductivity,[11] which are the main challenges in this system. There are several modifications that have been reported to enhance the catalytic activity and to obtain optimal performance of Ni for DUFC applications, such as structure modification to increase the surface area of the catalyst or by doping or combining with other metals (Ni-Co, Ni-Mn, Ni-Mo, etc).[13–17] Meanwhile, the use of porous catalysts is advantageous to overcome the slow reaction kinetics as they enhance the number of catalytic active sites for UOR due to their high catalytic surface area, affecting the reaction kinetics.[6]

Metal-organic frameworks (MOFs) have attracted great attention due to their tuneable structural properties. MOFs are porous crystals constructed of metal ions coordinated by polydentate organic ligands, forming one-, two-, or three-dimensional structures with large internal surface area, highly tuneable porosity, and the possibility of open metal sites.[18,19] MOFs can accommodate mixtures of metal ions in their structure, providing options for multifunctionality, and tuning the material properties to a specific application. Recent studies suggest that controlling the local electronic structures of mixed-metal centers and taking advantage of their synergistic effects could enhance the electrocatalytic activity of MOFs.[18] Owing to their excellent structural and electro-catalytic properties, MOFs have been used in the hydrogen evolution reaction, the oxygen evolution reaction, as well as in fuel cell applications.[20,21] Several studies have been reported for the use of Ni MOFs based catalysts in urea detection.[19,22] However, few reports are yet available on the use of Ni-based MOFs catalyst for urea/H_2O_2 fuel cell applications.[23]

In this paper, we study bimetallic NiCo MOF-74 crystallized at porous NiO (p-NiO) film. The bimetallic MOF with cobalt was selected to lower the formation potential of the NiOOH as the active sites of catalyst for UOR.[24,25] The use of p-NiO modified with NiCo MOF-74 shows an increase of electro-active surface area around five times that of nickel foil, and accordingly enhances the catalytic activity towards UOR. Further investigation of NiCo MOF-74 deposited at p-NiO (NiCo MOF-74@p-NiO) in a urea fuel cell system demonstrates superior performance, including enhanced current and power densities, as well as improved catalytic stability for long-time application.

METHODS

Synthesis of Ni, Co, and NiCo MOF-74 deposited at porous NiO

The p-NiO films were prepared based on our previous work.[26] A piece of nickel foil (99% purity with 0.3 mm thickness) was cleaned by sonication and an anodizing process was performed in ethylene glycol containing 2.0 wt.% water and 0.5 wt.% NH_4Cl using a standard two-electrode cell at 30 V for 15 min, followed by an annealing step at 400°C for 1 h. Characterization of the p-NiO performed using FTIR spectra revealed bands of 570 and 668 cm^{-1}, which were attributed to the vibrations of Ni-O and Ni-O-H, respectively.[26] UV-DRS observed an absorbance peak at around 414 nm, indicating the existence of nickel oxide, as this peak was not observed in the spectrum of the unmodified nickel foil.[26]

To synthesize Ni MOF-74, 0.991 g of $Ni(NO_3)_2 \cdot 6H_2O$ and 0.198 g of 2,5-dihydroxyterephthalic acid were dissolved in 20 mL DMF, ethanol, and water (v/v/v:1/1/1). The mixture was ultrasonicated for 30 min to form a homogenous solution before transferring to a 40 mL-Teflon-lined stainless-steel autoclave with a piece of nickel foil (1x1 cm^2) immersed into the mixture. The autoclave was placed into a fan oven and heated at 100 °C for 24 hours. After cooling to room temperature, the treated nickel was washed with methanol and deionized water several times and dried overnight at 60°C. The same procedure was applied to synthesize Co MOF-74, except for the use of 0.991 g of $Co(NO_3)_2$ $6H_2O$ as the source of metal, while Ni_1Co_1 MOF-74, Ni_3Co_2 MOF-74, and Ni_4Co_1 MOF-74 were synthesized using the same procedure with the metal sources of both $Ni(NO_3)_2$ $6H_2O$ and $Co(NO_3)_2$ $6H_2O$ in a various nickel-to-cobalt (Ni:Co) mole ratios of 1:1, 3:2, and 4:1, respectively.

The optimum ratio of Ni and Co was investigated by electrocatalytic measurements towards UOR using metal MOF-74 deposited onto the unmodified nickel foils. Once the ratio optimized, the metal MOF-74 with an optimum Ni:Co ratio was further synthesized onto the prepared p-NiO using the similar procedure. All the electrodes were characterized using powder XRD (Malvern Panalytical Empyrean diffractometer operating with Cu $K\alpha_{1/2}$ radiation) and SEM-EDX (Zeiss SUPRA 55-VP Field Emission Scanning Electron Microscope with an Oxford Instruments energy-dispersive X-ray detector) for confirmation of the MOF-74 formation.

UOR Electrochemical Measurements

The electrocatalytic performance towards UOR was measured using a potentiostat (Autolab, PGSTAT204) in 1.0 M KOH at room temperature (± 25 °C). A three-electrode system was used with MOF-modified p-NiO (surface area of 0.196 cm^2) as the working electrodes, Pt spiral as the counter electrode, and the Ag/AgCl (sat. KCl) as the reference electrode. Cyclic voltammetry (CV) and linear sweep voltammetry (LSV) was used to investigate the catalytic activity of each electrode sample. Chronoamperometry (CA) tests was also conducted to investigate the stability and durability of the electrodes.

Direct Urea Fuel Cells Tests

Investigation of the prepared electrodes for DUFCs was conducted using a two-chamber electrochemical cell test. The anode and cathode chambers were separated by a Nafion 115 membrane (DuPont). Prior to use, the membrane was pre-treated by boiling in 5% H_2O_2 and deionized water. All electrodes were connected to a potensiostat. Initially, open circuit voltage (OCV) was measured for 30 min until it reached the steady state. Then, current and power output

was measured by applying the collected OCV until it reached 0 V and the average of the last 10 seconds data in every 5 mins were recorded.

RESULT AND DISCUSSION

Optimization of NiCo MOF-74 ratio on Ni Foil

Fig. 1 shows the powder XRD patterns of all the prepared Ni, Co, and various NiCo MOF-74@Ni compared to the simulated pattern of MOF-74.[27] All samples show similar peak patterns to the simulated MOF-74 indicating successful synthesis at the surface of Ni foils. The two intense diffraction peaks at 7° and 12° in all patterns, indicate good crystallinity of the synthesized MOF-74 on the surface of Ni foil.[18,21] However, the relative peak intensities of the MOF-74 at higher angles are differ to that expected and this may be due to an oriented growth of the MOF at the surface. The lower crystallinity of the pure Co MOF-74 can also be noted, which may suggest that its' growth is not so effective at the Ni foil.

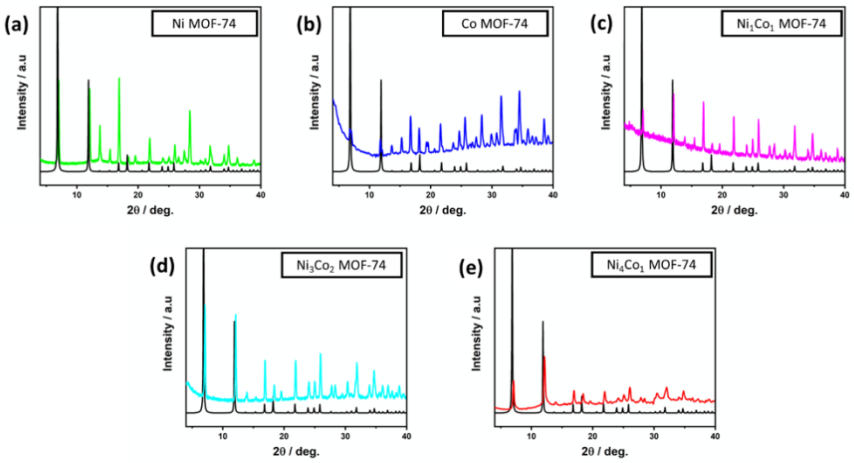

Figure 1 XRD patterns of Ni MOF-74@Ni (a), Co MOF-74@Ni (b), Ni_1Co_1 MOF-74@Ni (c), Ni_3Co_2 MOF-74@Ni (d), Ni_4Co_1 MOF-74@Ni (e), in comparison with that of the unmodified Ni foil (black lines of a-e).

The morphologies of the as-prepared electrodes were studied using SEM-EDX. Fig. 2 shows a typical SEM image of the unmodified Ni foil (Fig. 2a) in comparison with those of Ni MOF-74,

Co MOF-74, Ni_1Co_1 MOF-74, Ni_3Co_2 MOF-74, and Ni_4Co_1 MOF-74-deposited on Ni foils (Fig. 2b-f, respectively). The figure indicates that all metal MOF-74 with Ni-Co in all ratios fully cover the surface of the Ni foils. Significantly smaller particle sizes of Ni MOF-74 are observed compared to those of Co MOF-74, which can be explained by the difference in the crystallization kinetics between Ni MOF-74 and Co MOF-74.[28] A faster crystallization of Co MOF-74 is expected to occur and accordingly, the particle sizes of Ni MOF-74 are smaller than that of Co MOF-74. This phenomenon was also shown in all ratios of bimetallic NiCo MOF-74: larger particles were formed for Ni_1Co_1 MOF-74 (Fig. 2d) than Ni_4Co_1 MOF-74 (Fig. 2f) due to the lower concentration of cobalt in Ni_4Co_1 MOF-74.

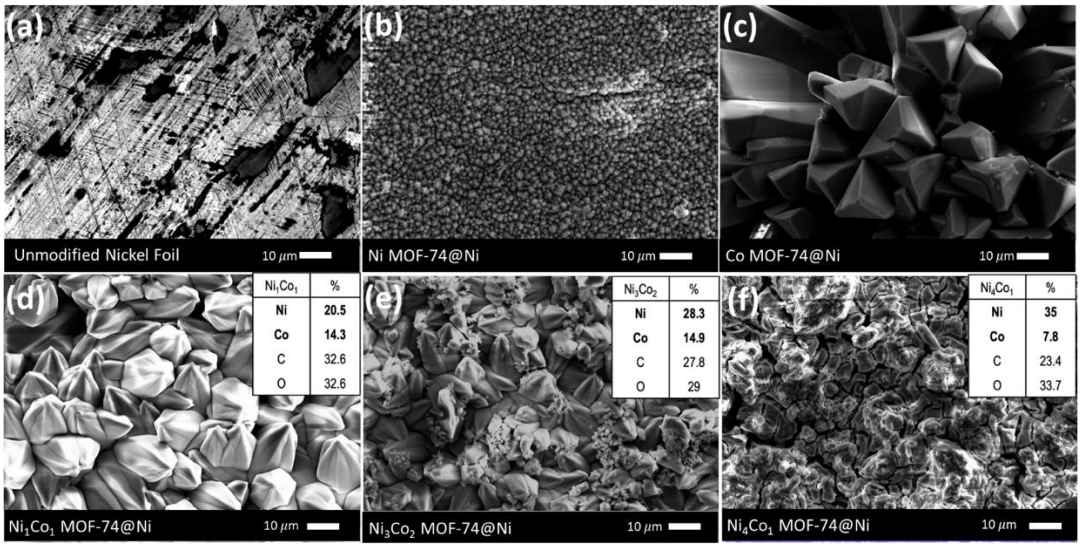

Figure 2 SEM-EDX images of the unmodified Ni foil (a), Ni MOF-74@Ni (b), Co MOF-74@Ni (c), Ni_1Co_1 MOF-74@Ni (d), Ni_3Co_2 MOF-74@Ni (e), and Ni_4Co_1 MOF-74@Ni (f)

EDX characterization was conducted to confirm the ratios of Ni and Co in the bimetallic NiCo MOF-74-deposited at Ni foils (NiCo MOF-74@Ni). The insets of Fig. 2 show the element compositions obtained from EDX results of all the prepared bimetallic NiCo MOF-74 samples. Ni_1Co_1, Ni_3Co_2, and Ni_4Co_1 show Ni:Co ratios of 1.4:1, 2:1, and 4.5:1, respectively, which are well compared with the initial synthesis ratios. Furthermore, EDX mapping of both Ni and Co

particles in MOF-74 in all ratios reveal a uniform elemental distribution on the surface Ni foils (Fig. S1).

An electrochemical study was conducted to evaluate the catalytic activity of all the prepared MOF-74@Ni towards urea electro-oxidation by employing CV in 1 M KOH in the presence and in the absence of 0.33 M urea. The voltammograms show that when using Co MOF-74@Ni as the electrode (Fig. 3a), reduction oxidation peak was not observed with and without the presence of urea. This result confirmed the inactive characteristic of cobalt for UOR as previously reported.[25,29]

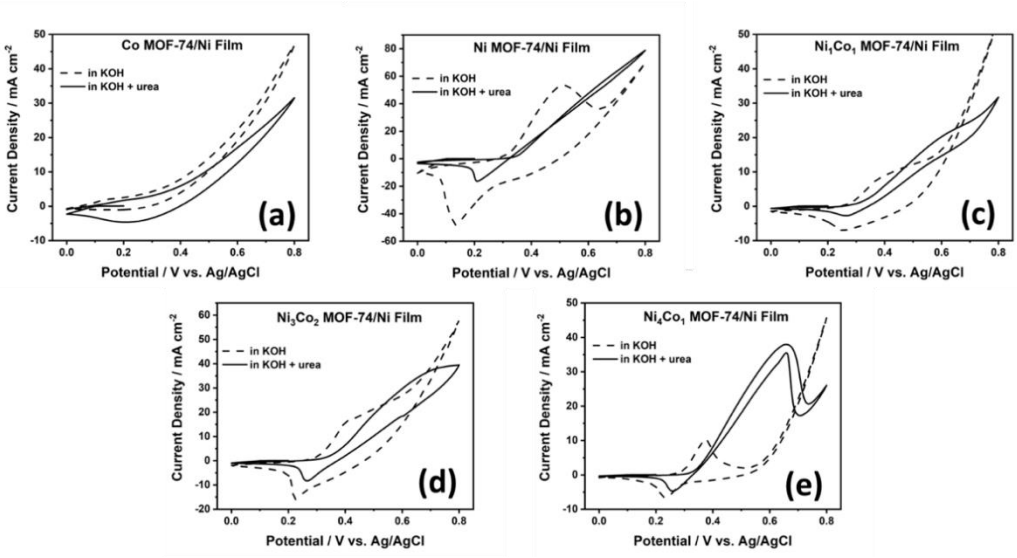

Figure 3 Cyclic voltammograms of Co MOF-74@Ni (a), Ni MOF-74@Ni (b), Ni_1Co_1 MOF-74@Ni (c), Ni_3Co_2 MOF-74@Ni (d), and Ni_4Co_1 MOF-74@Ni (e) in 1.0 M KOH in the presence (black line) and the absence (dash line) of 0.33 M urea.

However, the use of all the prepared MOF-74@Ni electrodes containing nickel in the absence of urea (Fig. 3b-e) show a typical oxidation and reduction couple peaks at +0.45 V and +0.2 V indicating the reversible conversion of $Ni(OH)_2$ (Ni^{2+}) to NiOOH (Ni^{3+}) in an alkaline system.[30] In the presence of urea, a significant increase of the reduction current at the onset potential of +0.3 V was observed at the prepared MOF-74@Ni electrodes containing nickel (Fig. 3b-e). In addition, an oxidation peak was detected at a potential of +0.6 V, which is attributed to the oxidation peak

of urea.[26] The observed peaks imply the contribution of NiOOH to the electro-oxidation reaction of urea,[31] indicating that the catalytic effect of nickel was still applicable although it is coordinated in the MOF-74 framework. However, the well-defined peak at +0.6 V could not be detected in Ni MOF-74@Ni, even though a significant increase in current density was observed. The absence of cobalt in the electrode was the probable reason and confirmed the contribution of cobalt in the film to decrease the oxidation potential of urea.[26]

To further evaluate the influence of Ni to Co ratios, comparison between signal-to-background current (S/B) ratios of the Ni and NiCo MOF-74@Ni with different Ni and Co ratios is summarized in Table 1. The table shows that the increase of cobalt content decreases the S/B ratios of the catalyst. The lowest S/B ratio was found when Ni MOF-74@Ni was used as the catalyst and was higher when cobalt replaced nickel in the samples. However, since cobalt is inactive for urea oxidation process, a higher cobalt content can cause a decrease of the S/B ratios. The same phenomenon was also found when the nickel and cobalt particles were deposited at carbon electrodes, confirming that the presence of cobalt could lower the potential needed to oxidize urea. [25,29] Accordingly, the Ni:Co ratio of 4:1 was selected for further experiments.

Table 1 Electrochemical performances of urea oxidation on various Ni:Co ratios of NiCo MOF-74@Ni electrodes

MOF-74 ratio	Background Current Density / mA cm^{-2}	Peak Current Density / mA cm^{-2}	Signal-to-Background Current Ratio
Ni	53.33	78.84	0.48
Ni_1Co_1	8.90	20.16	1.26
Ni_3Co_2	15.47	35.79	1.31
Ni_4Co_1	10.13	35.50	2.50

Synthesis of Ni_4Co_1 MOF-74 on porous NiO film

Powder XRD of the Ni_4Co_1 MOF-74 synthesized onto the surface of p-NiO (Ni_4Co_1 MOF-74@p-NiO) is well compared to the simulated Ni MOF-74 and Co MOF-74, implying that a high crystallinity of Ni_4Co_1 MOF-74 on p-NiO (Fig. 4a). Further confirmation using SEM-EDX (Fig. 4b) shows a uniform elemental distribution with full coverage of NiCo MOF-74 particles on the surface of p-NiO. A composition of 26.9% Ni, 7.3% Co, 31.8% C and 33.9% O was obtained, confirming the Ni:Co ratio of 4:1 of the NiCo MOF-74 at the surface of p-NiO.

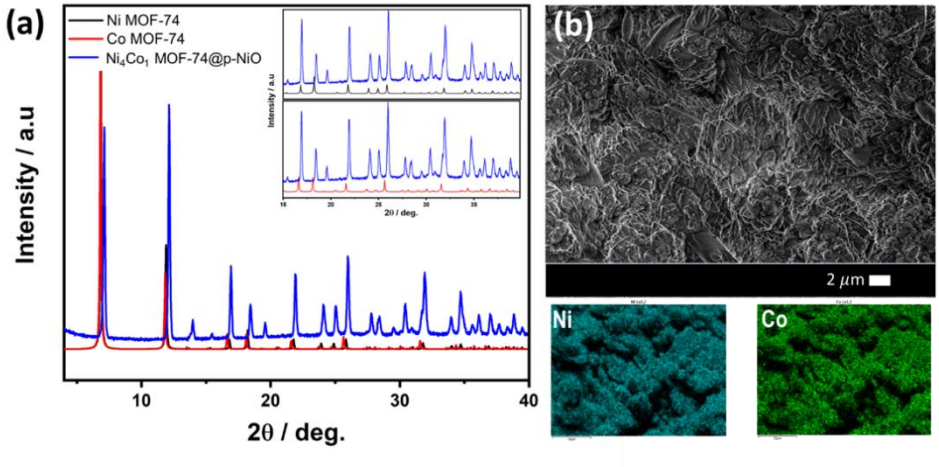

Figure 4 (a) XRD peak pattern of Ni_4Co_1 MOF-74@p-NiO in compared with those of Ni MOF-74@p-NiO and Co MOF-74@p-NiO and (b) SEM-images of Ni_4Co_1 MOF-74@p-NiO with its EDX mapping.

Electrochemical study of Ni4Co1 MOF-74@pNiO

A standard inorganic potassium ferro- and ferricyanide solution was used to evaluate the electro-active surface area of Ni_4Co_1 MOF-74@p-NiO compared to the unmodified Ni foil, p-NiO, and Ni_4Co_1@p-NiO.[32] The voltammograms of all electrodes (Fig. 5) show a coupled peak, attributed to the oxidation reduction peaks of iron at potentials of around +0.3 V and +0.2 V. All

the current peaks on all electrodes increased with the increase of the scan rates. Subsequently, the electro-active surface area was determined by the Randles-Sevcik equation as follows[33]:

$$\boldsymbol{i_p = 2.687\ x\ 10^5 n^{\frac{3}{2}} A D^{\frac{1}{2}} C v^{\frac{1}{2}}} \quad (1)$$

Where $\boldsymbol{i_p}$ is the peak current, $\boldsymbol{n}$ is the number of electrons transferred ($\boldsymbol{n}$ =1), $\boldsymbol{A}$ is the electrode surface area, $\boldsymbol{D}$ is the diffusion coefficient (6.5 x 10^{-6} cm^2 s^{-1}), $\boldsymbol{C}$ is the concentration of the used redox solution, and $\boldsymbol{v}$ is the scan rate.

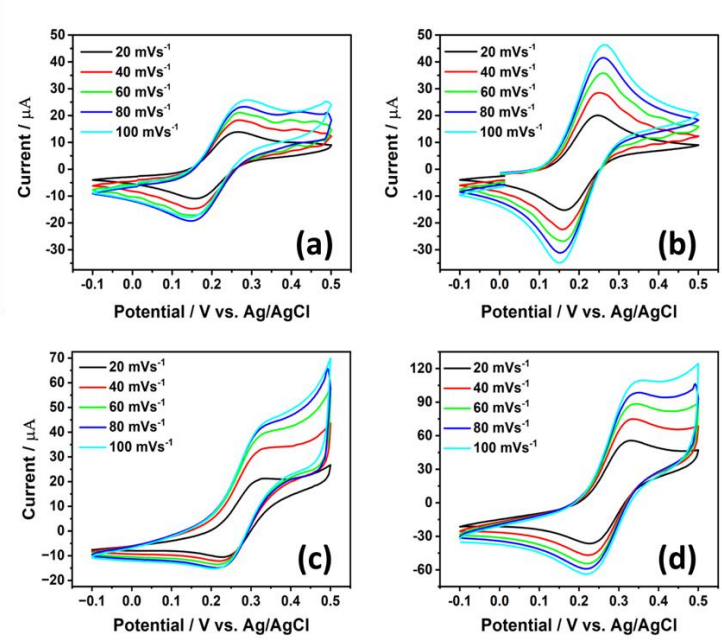

Figure 5 Cyclic voltammograms of the unmodified Ni (a), p-NiO (b), Ni_4Co_1@pNiO (c), and Ni_4Co_1 MOF-74@p-NiO (d) in a 1 mM $K_4Fe(CN)_6$ solution recorded at different scan rates.

Table 2 summarizes the electro-active surface areas calculated from the data in Fig. 5. The p-NiO electrode shows around two times higher of the electro-active surface area compared to the unmodified nickel foil due to its porous structure, while modification with Ni_4Co_1 MOF-74 at p-NiO increased the surface-active area to about five times higher than the unmodified nickel foil.

Therefore, the catalytic activity enhancement for UOR at by the modification of p-NiO with Ni_4Co_1 MOF-74 is expected.

Table 2 Summary of the related active surface areas calculated by Randles-Sevcik equation on the unmodified Ni foil, p-NiO, Ni_4Co_1@pNiO, and Ni_4Co_1 MOF-74@p-NiO, extracted from Fig. 5.

Catalyst	Linear Equation	Correlation, R^2	Electro-active surface area (cm^2)
Unmodified Ni foil	y = 69.67x + 4.13	0.99	0.11
p-NiO	y = 154.35x – 1.99	0.99	0.23
Ni_4Co_1@p-NiO	y = 145.32x + 2.95	0.96	0.21
Ni_4Co_1 MOF-74@p-NiO	y = 400.43x + 3.44	0.99	0.53

Electrochemical studies on the UOR were carried out at Ni_4Co_1 MOF-74@p-NiO compared to the unmodified Ni, p-NiO, and Ni_4Co_1@p-NiO using LSV in 1.0 M KOH electrolyte with and without the addition of 0.33 M urea. An oxidation peak at a potential of around +0.4 V was observed at all electrodes, which was attributed to the oxidation of $Ni(OH)_2$ (Ni^{2+}) to NiOOH (Ni^{3+}) in an alkaline system.[30] The voltammograms (Fig. 6) also show an increase in the current density at all electrodes. The highest current density was observed at Ni_4Co_1 MOF-74@p-NiO (35.79 mA cm^{-2}) compared to Ni foil (1.62 mA cm^{-2}), p-NiO (7.16 mA cm^{-2}), and Ni_4Co_1@p-NiO (25.78 mA cm^{-2}), indicating the highest catalytic activity of Ni_4Co_1 MOF-74@p-NiO towards UOR. The voltammogram was also measured for Ni_4Co_1 MOF-74 crystallized on carbon foam (CF) to see the influence of the supporting electrode (Fig. S3). Unlike the voltammogram for Ni_4Co_1 MOF-74@p-NiO electrode, the oxidation peak was not observed for Ni_4Co_1 MOF-74@CF either in the absence or the presence of urea. This is likely to be because a higher potential is needed to perform the oxidation reaction of Ni and urea on carbon foam as it has no catalytic

activity for urea oxidation, as well as a lower conductivity than nickel foam. Therefore, the use of p-NiO as the supporting electrode has been proven to show excellent activity towards UOR. Further observation of the onset potential of UOR at Ni_4Co_1 MOF-74@p-NiO revealed a left shift compared to other electrodes. In the presence of urea, the unmodified nickel foil electrode has an onset potential of 0.39 V (vs. Ag/AgCl), which was close to those of p-NiO and Ni_4Co_1@p-NiO at 0.38 V (vs. Ag/AgCl). However, a significant potential decrease was shown by Ni_4Co_1 MOF-74@p-NiO at 0.27 V vs. (Ag/AgCl), confirming that the modification of p-NiO with Ni_4Co_1 MOF-74 decreases the onset potential required by the electrode to initiate the urea oxidation process.

Tafel slope analysis of the four electrodes (Fig. 6c) was performed to evaluate the reaction kinetics of their catalytic activity. A low Tafel slope implies fast reaction kinetics at the electrode surface.[6] Ni_4Co_1 MOF-74@p-NiO showed the lowest Tafel slope (39.00 mV dec^{-1}), compared to Ni foil (55.37 mV dec^{-1}), p-NiO (41.93 mV dec^{-1}), and Ni_4Co_1@p-NiO (176.86 mV dec^{-1}). This indicates an increase in urea electro-oxidation reaction rate at the NiCo MOF-74@p-NiO surface, along with the increase in applied overpotential.[34] The highest Tafel slope value obtained for the Ni_4Co_1@p-NiO electrode, may be due to the less porous nature of the NiCo particles that inhibit the urea electro-oxidation reaction. This also proves that the modification with bimetallic MOF-74 structure increases the surface area of p-NiO as high porosity MOF-74 can facilitate the oxidation of urea with more catalytic active sites and accelerate the electro-oxidation process of urea. A Summary of the electrochemical analysis of the four electrodes towards UOR are presented in Table 3. In addition, compared to other recent developed catalysts for UOR, Ni_4Co_1 MOF-74 also showed a low and comparable onset potential and Tafel slope result making this developed electrode a very promising catalyst for UOR.[35–37]

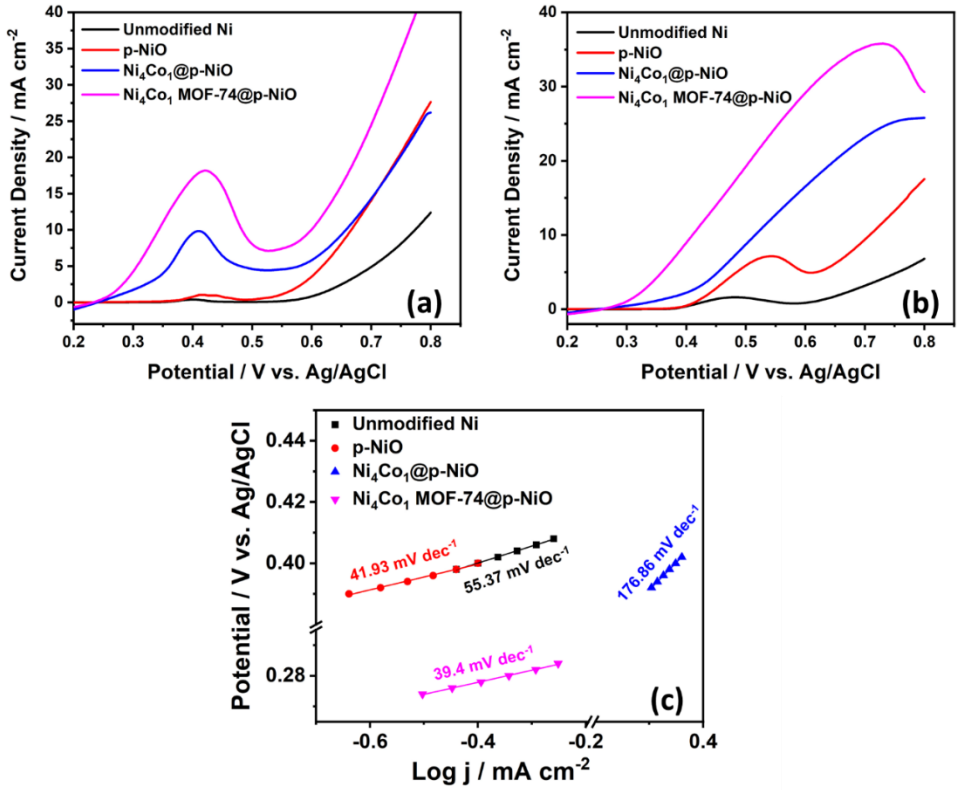

Figure 6 Voltammograms of the unmodified Ni foil, p-NiO, Ni_4Co_1@pNiO, and Ni_4Co_1 MOF-74@p-NiO electrodes in 1.0 M KOH in the absence (a) and the presence (b) of 0.33 M urea and their related Tafel plots (c)

Table 3 Electrochemical parameters of the studied electrodes towards UOR. The data were extracted from Fig. 6.

Catalyst	Current Density (mA cm^{-2})	Onset Potential (V vs. Ag/AgCl)	Tafel Slope (mV dec^{-1})
Unmodified Ni	1.167	0.39	55.37
p-NiO	7.164	0.39	41.93
Ni_4Co_1@p-NiO	25.785	0.40	176.86
Ni_4Co_1 MOF-74@p-NiO	35.788	0.31	39.40

Voltammograms of Ni_4Co_1 MOF-74@p-NiO were examined in various concentrations of KOH and urea to determine the optimum electrolyte concentration for the DUFC applications. The voltammograms of Ni_4Co_1 MOF-74@p-NiO in 0.33 M urea with various concentrations of KOH (Fig. 7a) show that the increase of KOH concentrations in the UOR decreases the onset potential of NiOOH formation, thereby increasing the current density. The probable reason is the presence of more OH^- ions accelerate the formation of NiOOH species in the lower potential.[15,38]

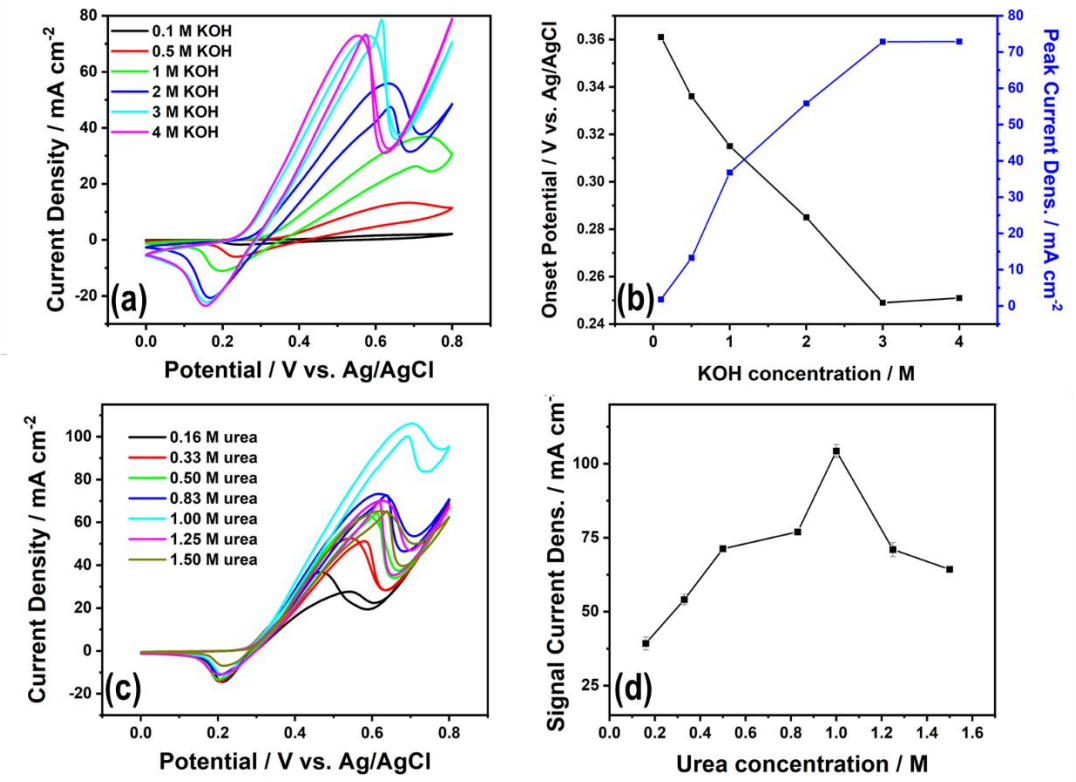

Figure 7 Voltammograms of Ni_4Co_1 MOF-74@-p-NiO (a) in 0.33 M urea at different concentrations of KOH and (b) the effect on the peak current density and the onset potential (b), together with (c) voltammograms at different concentration of urea in 0.1 M KOH and (d) the effect of urea concentration on peak current density

Plots of the onset potentials and current densities versus KOH concentrations in Fig. 7b show that the increase of current density and the decrease of the onset potential with the increase of KOH concentration reaches maximum at 3 M and remain stable at a concentration of 4 M KOH.

This is probably because the increase of the solution viscosity with the KOH concentration (containing 0.33 M urea) inhibits the charge transfer and blocks the catalytic sites.[5] In addition, the oxygen evolution reaction and the accumulation of other unwanted products might occur in high KOH concentrations leading to block the diffusion of urea and decreasing the performance of UOR.[39] Accordingly, the concentration of 3 M KOH was set for the remaining experiments.

Urea concentration was optimized at 3 M KOH concentration. Fig. 7c shows the cyclic voltammogram of the Ni_4Co_1 MOF-74@p-NiO electrode at various urea concentrations. The plots of current density with urea concentration show that the current increase reaches its maximum at 1.0 M, indicating the saturation kinetics of UOR on Ni_4Co_1 MOF-74@p-NiO. At the higher concentrations, the excess of urea might cover the surface of the electrode to limit the contact with OH- and suppress NiOOH formation, the active catalyst for UOR.[15] Meanwhile, at lower concentrations, the obtained current density was low due to insufficient amount of urea to optimize UOR performance. Based on the results, 3.0 M KOH concentration and 1.0 M urea concentration were used in the following experiments.

Stability and repeatability tests were carried out on the Ni_4Co_1 MOF-74@p-NiO electrodes using chronoamperometry at 0.55 V for 1 hour and LSV for five times tests. SEM-EDX and XRD characterization was also conducted on the sample electrodes after the CA and LSV test to examine the stability of the modified Ni_4Co_1 MOF-74 on the surface of p-NiO. Chronoamperograms of Ni_4Co_1 MOF-74@p-NiO in 3.0 M KOH (Fig. 8a) in the absence of urea show a stable current density of Ni_4Co_1 MOF-74@p-NiO at an applied potential of 0.55 V for 1 hour. In the presence of 1.0 M urea higher current density values with an average value of 43 mA cm^{-2} was obtained. Good stability of the current was also observed, indicating a stable UOR processes occurred on the surface of the Ni_4Co_1 MOF-74@p-NiO.

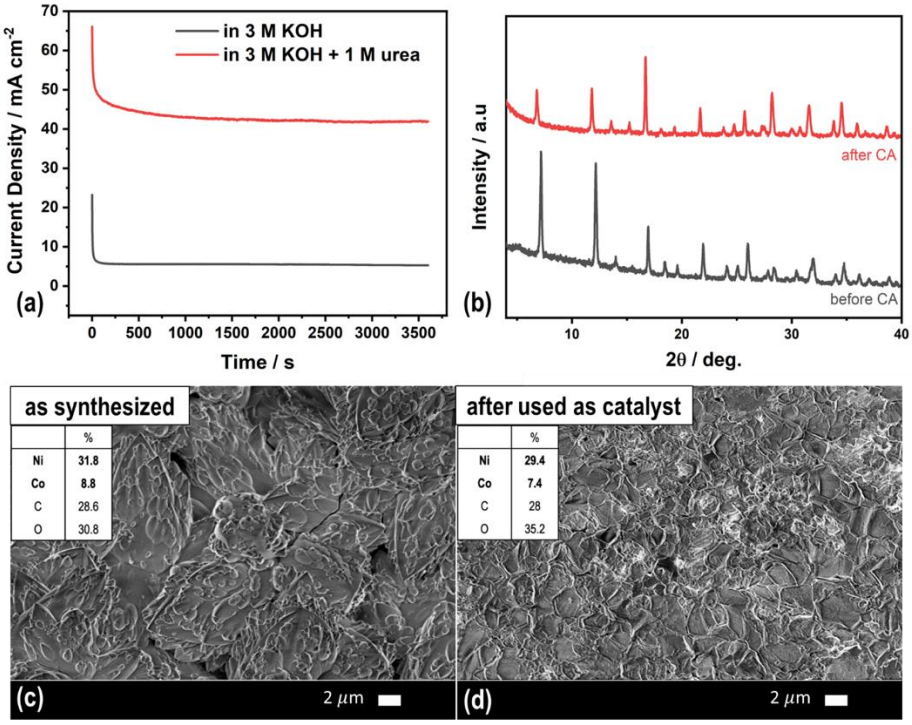

Figure 8 (a) Chronoamperograms Ni_4Co_1 MOF-74@p-NiO in 3.0 M KOH in the absence and in the presence of 1.0 M urea at an applied potential of 0.55 V for one hour; (b) the XRD pattern before-after the CA test, and SEM-EDX (c) before and (d) after the chronoamperometry test.

XRD patterns of Ni_4Co_1 MOF-74@p-NiO carried out before and after the stability test (Fig. 8b) show no significant difference on the peak patterns. However, a slight decrease in the peak intensity was observed, which may be due to the removal of any loosely bound Ni_4Co_1 MOF-74 on the surface of p-NiO to leave the well-attached layer. EDX characterization (Fig. 8c and 8d) shows the same percentage of the remain elements, confirming that Ni_4Co_1 MOF-74 is stable on the surface of p-NiO.

Repeatability tests were also carried out using LSV in 3.0 M KOH with the addition of 1.0 M urea for five times measurements. Twenty scans of the LSV test were performed until a stable current density was obtained (Fig. 9a). This shows that peak current density as well as the S/B

ratio was stable without any significant change during the five times-repeatability tests. The repeatability performance of Ni_4Co_1 MOF-74@p-NiO for 5-times repeatability tests is summarized in Fig. S4 and Table S1, implying that this developed Ni_4Co_1 MOF-74@p-NiO is promising to be used as UOR electrode for long-time application.

Fig. 9b shows the powder XRD patterns of Ni_4Co_1 MOF-74@p-NiO before and after each repeatability test from the first to the fifth measurement. The characteristic peaks of Ni_4Co_1 MOF-74 are observed after repeatability test confirming the existence of Ni_4Co_1 MOF-74 on the surface of p-NiO. Again, the initial decrease in the peak intensity may be due to the removal of unattached Ni_4Co_1 MOF-74 particles at the p-NiO surface. However, once the excess particles are removed, the NiCo MOF-74 remained stable on the p-NiO surface in remaining LSV cycles. Confirmation was performed using UV-vis spectral characterization of the solution suggesting the dissolution of Ni and Co particles into the electrolyte (Fig. S2). Another possibility of the peak decrease is tapping of molecules formed during the UOA process (the presence of CO_2, N_2, or even urea itself) in the porous of MOF-74 structure. However, further characterization is needed to further elaborate this phenomenon. Nonetheless, the intensity was observed to be stable after the 3^{rd} to 5^{th} day of testing.

Characterization using SEM-EDX, Fig. 9c and 9d, show the existence of Ni_4Co_1 MOF-74 particles on the p-NiO surface. However, we observed the increase of Ni percentage after the repeatability test from 4:1 to 7:1 (Table S2). This decrease might be due to the loss of Ni4Co1 MOF-74 leading to more exposed Ni film detected by the EDX and increases the percentage of Ni elements on the surface of the Ni_4Co_1 MOF-74@p-NiO.

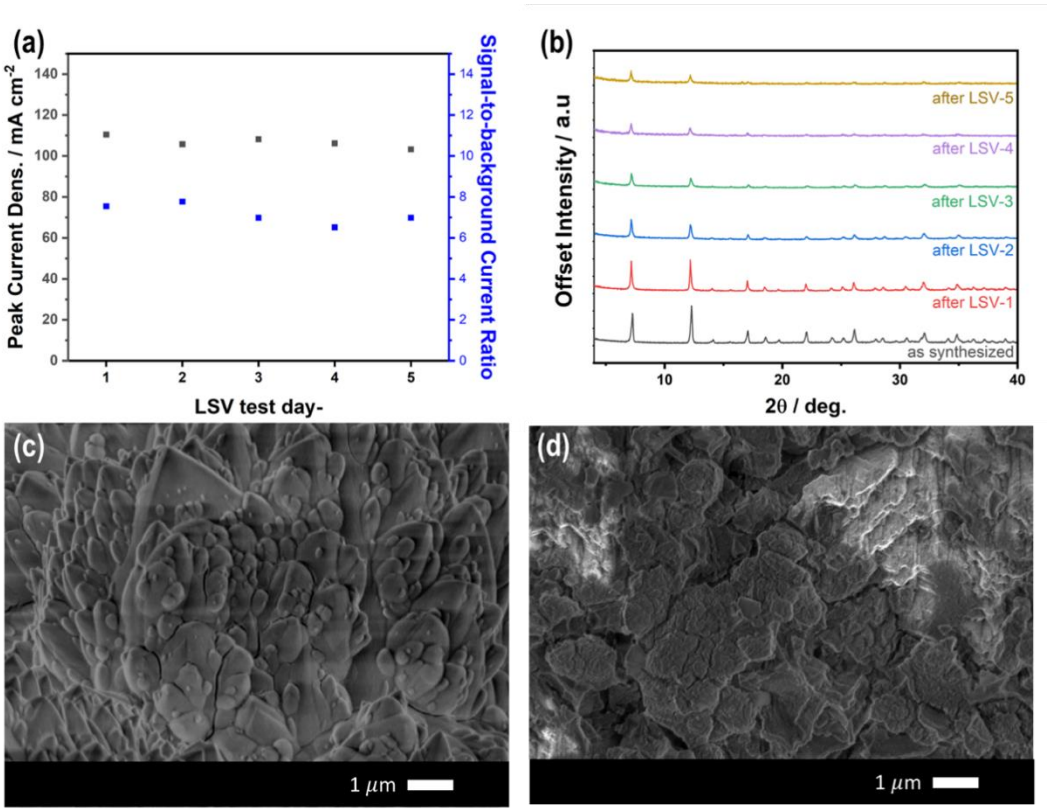

Figure 9 (a) The curve of peak current density as well as signal-to-background current ratio vs. the number linear sweep voltammetry performed at Ni_4Co_1 MOF-74@p-NiO together with (b) XRD pattern before and after the tests, and SEM images (c) before and (d) after the repeatability tests.

Direct Urea Fuel Cell Application

DUFC testing was conducted in a two-chamber fuel cell using the Ni_4Co_1 MOF-74@p-NiO as the anode with Pt spiral as the cathode. The activity of Ni_4Co_1 MOF-74@p-NiO in the DUFC was also compared with those of the unmodified Ni foil, p-NiO, and Ni_4Co_1@p-NiO (Fig. 10a). The better performance of both p-NiO and Ni_4Co_1@p-NiO (in terms of current density, power density, and potential) than that of the unmodified Ni foil was observed as expected, due to the porous structure on the surface of p-NiO. In addition, modification with bimetallic Ni-Co particles on p-NiO improved the performance of UOR in the DUFC by lowering the formation potential of

NiOOH. However, Ni_4Co_1@p-NiO showed slightly lower performances, which is consistent with its high Tafel slope value described above. This phenomenon was also confirmed by the smaller electro-active surface area of Ni_4Co_1@p-NiO (0.212 cm^2), compared to the p-NiO (0.225 cm^2).

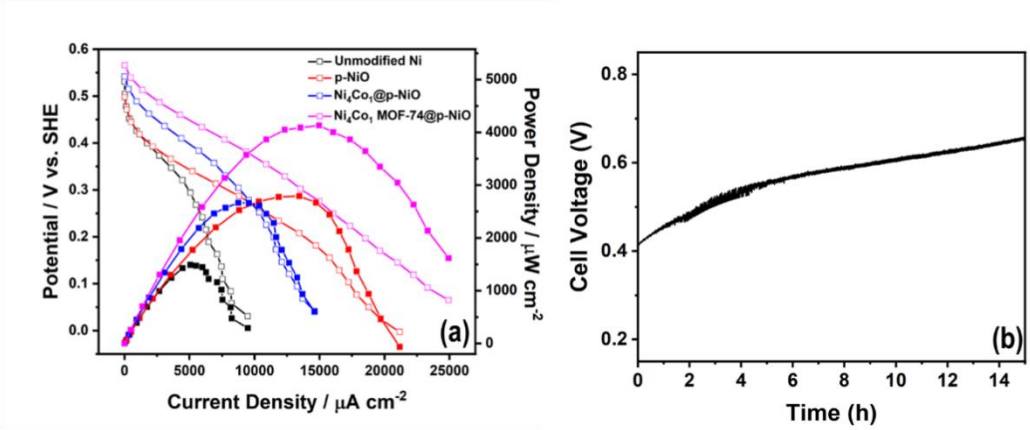

Figure 10 The performance of urea/H_2O_2 fuel cell using NiCo MOF-74@p-NiO in comparison with other electrodes (a) and its potential versus time during 15 h test at a current density of 10 mA cm^{-2} (b)

Ni_4Co_1 MOF-74@p-NiO was observed to produce the optimum performance compared to all electrodes (Table 4), suggesting that the modification of p-NiO surface with Ni_4Co_1 MOF-74 is the most suitable to improve the DUFC performance. The performance is also consistent with the obtained electro-active surface area of Ni_4Co_1 MOF-74@p-NiO (0.534 cm^2), which is five times larger than the nickel foil. This result implies that the high porosity of the modifying MOF is the main factor to increase the active surface area and availability of catalytic active sites of the electrodes, resulting in the acceleration of the electro-oxidation urea. Comparison with previously reported anodes applied in typical direct urea fuel cells is presented in Table 4. It can be seen that the Ni_4Co_1 MOF-74@p-NiO gives a higher maximum power density than almost all the other materials reported that have been studied under similar conditions. Although a better performance was shown by nickel cobalt-modified nanowire arrays, this was probably due to the use of very

high concentration of KOH in that study. This would be difficult to apply with porous electrodes, as the increased viscosity will hinder mass transfer.

Examination on the stability of the urea fuel cell using NiCo MOF-74@p-NiO as the anode using the two-chamber fuel cell was also performed at a current density of 10 mA cm^{-2} for 15 hours. Fig. 10b shows the cell voltage was increased until ~0.6 V, indicating the excellent performance of the NiCo MOF-74@p-NiO as the anode.

Table 4 Comparison of the performances of different reported anode catalysts in the urea/H_2O_2 fuel cell test.

Anode	Cathode	Fuel	Oxidant	Max. Power Density ($mW\ cm^{-2}$)
Unmodified Ni foil	Pt	3 M KOH + 1 M urea	2 M H_2O_2 + 2 M H_2SO_4	1.488
p-NiO				2.792
Ni_4Co_1@p-NiO				2.608
Ni_4Co_1 MOF-74@p-NiO				4.131
Ni/MWCNTs[7]	Pt/C	1.0 M urea + 1.5 M NaOH	20 % H_2O_2 + 5% H_3PO_4	0.06
Ni_4Co_1/C[25]	Pt Foil	0.33 M urea	Humidified Oxygen	1.57
NiCo NWAs[2]	Pd/CFC	0.33 M urea + 9 M KOH	2 M H_2O_2 + 2 M H_2SO_4	7.40
NiCo-BDD[31]	Pt spiral	0.5 M urea + 0.1 M KOH	2 M H_2O_2 + 2 M H_2SO_4	0.63

CONCLUSION

NiCo MOF-74 has been crystallized at the surface of anodized porous NiO using a solvothermal method. A Ni-to-Co ratio of 4:1 showed the highest current density as well as signal-to-background current ratio towards urea electro-oxidation reaction with a five-times electro-active surface area

higher than that of the nickel foil. A current density of 110 mA cm^{-2} could be achieved for urea oxidation reaction in 3 M KOH containing 1 M urea with a good stability for 1 hour and five-times repeatability measurements. The application of the NiCo MOF-74@p-NiO as an anode in the direct urea fuel cell showed an enhancement of power density in comparison with those of the unmodified nickel foil and anodized NiO porous film. An excellent stability for 15 hours application was also observed, indicating that the material is promising for a real direct urea fuel cell.

ASSOCIATED CONTENT

Supporting Information. The following files are available free of charge. Referenced data Figure S1-S3 detailed the mapping distribution of the synthesized NiCo MOF-74, UV Vis characterization, and the LSV curve repeatability performance. Referenced data Table S1 and S2 detailed the repeatability performance and EDX characterization before and after the repeatability performance.

AUTHOR INFORMATION

Corresponding Author

Tribidasari A. Ivandini and Richard I. Walton

Email: ivandini.tri@sci.ui.ac.id and R.I.Walton@warwick.ac.uk

Author Contributions

YMTAP: data curation, formal analysis, investigation, and writing; TWC: data curation, investigation, validation; VD: conceptualization, supervision; JG: conceptualization, supervision, validation; YKK: supervision and validation; RIW: conceptualization,

supervision, validation, writing–review & editing; TAI: conceptualization, supervision, validation, funding acquisition, writing–review & editing. All authors have given approval to the final version of the manuscript.

Funding Sources

This work was partly funded by PKPI PMDSU Kemenristek Dikti 2021. Contract No. 170.7/E4.4/KU/2021. We are also grateful to the British Council for providing funding via a Newton Fund Institutional Links project (527290660).

Notes

The authors declare that they have no competing interests.

ACKNOWLEDGMENT

We would like to thank Katie Pickering, Mark, and Jasmine Clayton for their help in carrying the SEM and XRD in this work. Some of the equipment used was provided by the University of Warwick's Research Technology Platforms.

REFERENCES

(1) Fan, Z.; Kwon, Y. H.; Yang, X.; Xu, W.; Wu, Z. In-Situ Production of Hydrogen Peroxide as Oxidant for Direct Urea Fuel Cell. In *Energy Procedia*; Elsevier Ltd, 2017; Vol. 105, pp 1858–1863. https://doi.org/10.1016/j.egypro.2017.03.544.

(2) Guo, F.; Cheng, K.; Ye, K.; Wang, G.; Cao, D. Preparation of Nickel-Cobalt Nanowire Arrays Anode Electro-Catalyst and Its Application in Direct Urea/Hydrogen Peroxide Fuel Cell. *Electrochim Acta* **2016**, *199*, 290–296. https://doi.org/10.1016/j.electacta.2016.01.215.

(3) Ye, K.; Wang, G.; Cao, D.; Wang, G. Recent Advances in the Electro-Oxidation of Urea for Direct Urea Fuel Cell and Urea Electrolysis. *Topics in Current Chemistry*. 2018, pp 42–78. https://doi.org/10.1007/s41061-018-0219-y.

(4) Rollinson, A. N.; Jones, J.; Dupont, V.; Twigg, M. v. Urea as a Hydrogen Carrier: A Perspective on Its Potential for Safe, Sustainable and Long-Term Energy Supply. *Energy Environ Sci* **2011**, *4* (4), 1216–1224. https://doi.org/10.1039/c0ee00705f.

(5) Guo, F.; Cao, D.; Du, M.; Ye, K.; Wang, G.; Zhang, W.; Gao, Y.; Cheng, K. Enhancement of Direct Urea-Hydrogen Peroxide Fuel Cell Performance by Three-Dimensional Porous Nickel-Cobalt Anode. *J Power Sources* **2016**, *307*, 697–704. https://doi.org/10.1016/j.jpowsour.2016.01.042.

(6) Abdel Hameed, R. M.; Medany, S. S. Enhanced Electrocatalytic Activity of NiO Nanoparticles Supported on Graphite Planes towards Urea Electro-Oxidation in NaOH Solution. *Int J Hydrogen Energy* **2017**, *42* (38), 24117–24130. https://doi.org/10.1016/j.ijhydene.2017.07.236.

(7) Serban, E. C.; Balan, A.; Iordache, A. M.; Cucu, A.; Ceaus, C.; Necula, M.; Ruxanda, G.; Bacu, C.; Mamut, E.; Stamatin, I. Urea/ Hydrogen Peroxide Fuel Cell. *Dig J Nanomater Biostruct* **2014**, *9* (4), 1647–1654.

(8) Lan, R.; Tao, S. Preparation of Nano-Sized Nickel as Anode Catalyst for Direct Urea and Urine Fuel Cells. *J Power Sources* **2011**, *196* (11), 5021–5026. https://doi.org/10.1016/j.jpowsour.2011.02.015.

(9) Wu, N.; Zhang, X.; Guo, R.; Ma, M.; Zhang, Y.; Hu, T. Nickel Nanocrystal/Sulfur-Doped Carbon Composites as Efficient and Stable Electrocatalysts for Urea Oxidation Reaction. *J Alloys Compd* **2022**, *903*, 163916. https://doi.org/10.1016/j.jallcom.2022.163916.

(10) Ao, X.; Gu, Y.; Li, C.; Wu, Y.; Wu, C.; Xun, S.; Nikiforov, A.; Xu, C.; Jia, J.; Cai, W.; Ma, R.; Huo, K.; Wang, C. Sulfurization-Functionalized 2D Metal-Organic Frameworks for High-Performance Urea Fuel Cell. *Appl Catal B* **2022**, *315*, 121586. https://doi.org/10.1016/j.apcatb.2022.121586.

(11) Yan, W.; Wang, D.; Botte, G. G. Nickel and Cobalt Bimetallic Hydroxide Catalysts for Urea Electro-Oxidation. *Electrochim Acta* **2012**, *61*, 25–30. https://doi.org/10.1016/j.electacta.2011.11.044.

(12) Wang, D.; Botte, G. G. In Situ X-Ray Diffraction Study of Urea Electrolysis on Nickel Catalysts. *ECS Electrochemistry Letters* **2014**, *3* (9), 29–32. https://doi.org/10.1149/2.0031409eel.

(13) Li, Q.; Li, N.; An, J.; Pang, H. Controllable Synthesis of a Mesoporous NiO/Ni Nanorod as an Excellent Catalyst for Urea Electro-Oxidation. *Inorg Chem Front* **2020**, *7* (10), 2089–2096. https://doi.org/10.1039/d0qi00316f.

(14) Alex, C.; Shukla, G.; John, N. S. Introduction of Surface Defects in NiO with Effective Removal of Adsorbed Catalyst Poisons for Improved Electrochemical Urea Oxidation. *Electrochim Acta* **2021**, *385*, 138425. https://doi.org/10.1016/j.electacta.2021.138425.

(15) Tesfaye, R. M.; Das, G.; Park, B. J.; Kim, J.; Yoon, H. H. Ni-Co Bimetal Decorated Carbon Nanotube Aerogel as an Efficient Anode Catalyst in Urea Fuel Cells. *Sci Rep* **2019**, *9*, 479. https://doi.org/10.1038/s41598-018-37011-w.

(16) Liu, Y.; Shu, C.; Fang, Y.; Chen, Y.; Liu, Y. Two 3D Structured Co-Ni Bimetallic Oxides as Cathode Catalysts for High-Performance Alkaline Direct Methanol Fuel Cells. *J Power Sources* **2017**, *361*, 160–169. https://doi.org/10.1016/j.jpowsour.2017.06.062.

(17) Barakat, N. A. M.; El-Newehy, M. H.; Yasin, A. S.; Ghouri, Z. K.; Al-Deyab, S. S. Ni&Mn Nanoparticles-Decorated Carbon Nanofibers as Effective Electrocatalyst for Urea Oxidation. *Appl Catal A Gen* **2016**, *510*, 180–188. https://doi.org/10.1016/j.apcata.2015.11.015.

(18) Zhang, M.; Xu, W.; Li, T.; Zhu, H.; Zheng, Y. In Situ Growth of Tetrametallic FeCoMnNi-MOF-74 on Nickel Foam as Efficient Bifunctional Electrocatalysts for the Evolution Reaction of Oxygen and Hydrogen. *Inorg Chem* **2020**, *59* (20), 15467–15477. https://doi.org/10.1021/acs.inorgchem.0c02504.

(19) Tran, T. Q. N.; Das, G.; Yoon, H. H. Nickel-Metal Organic Framework/MWCNT Composite Electrode for Non-Enzymatic Urea Detection. *Sens Actuators B Chem* **2017**, *243*, 78–83. https://doi.org/10.1016/j.snb.2016.11.126.

(20) Meng, C.; Cao, Y.; Luo, Y.; Zhang, F.; Kong, Q.; Alshehri, A. A.; Alzahrani, K. A.; Li, T.; Liu, Q.; Sun, X. A Ni-MOF Nanosheet Array for Efficient Oxygen Evolution Electrocatalysis in Alkaline Media. *Inorg Chem Front* **2021**, *8* (12), 3007–3011. https://doi.org/10.1039/d1qi00345c.

(21) Li, S.; Zhu, X.; Yu, H.; Wang, X.; Liu, X.; Yang, H.; Li, F.; Zhou, Q. Simultaneous Sulfamethoxazole Degradation with Electricity Generation by Microbial Fuel Cells Using Ni-MOF-74 as Cathode Catalysts and Quantification of Antibiotic Resistance Genes. *Environ Res* **2021**, *197*, 111054. https://doi.org/10.1016/j.envres.2021.111054.

(22) Bao, C.; Niu, Q.; Chen, Z. A.; Cao, X.; Wang, H.; Lu, W. Ultrathin Nickel-Metal-Organic Framework Nanobelt Based Electrochemical Sensor for the Determination of Urea in Human Body Fluids. *RSC Adv* **2019**, *9* (50), 29474–29481. https://doi.org/10.1039/c9ra05716a.

(23) Tran, T. Q. N.; Park, B. J.; Yun, W. H.; Duong, T. N.; Yoon, H. H. Metal–Organic Framework–Derived Ni@C and NiO@C as Anode Catalysts for Urea Fuel Cells. *Sci Rep* **2021**, *10* (1), 278. https://doi.org/10.1038/s41598-019-57139-7.

(24) Vidotti, M.; Silva, M. R.; Salvador, R. P.; Torresi, S. I. C. de; Dall'Antonia, L. H. Electrocatalytic Oxidation of Urea by Nanostructured Nickel/Cobalt Hydroxide Electrodes. *Electrochim Acta* **2008**, *53* (11), 4030–4034. https://doi.org/10.1016/j.electacta.2007.11.029.

(25) Xu, W.; Zhang, H.; Li, G.; Wu, Z. Nickel-Cobalt Bimetallic Anode Catalysts for Direct Urea Fuel Cell. *Sci Rep* **2014**, *4*, 5863. https://doi.org/10.1038/srep05863.

(26) Putri, Y. M. T. A.; Gunlazuardi, J.; Ivandini, T. A. Electrochemical Preparation of Highly Oriented Microporous Structure Nickel Oxide Films as Promising Electrodes in Urea Oxidation. *Chem Lett* **2022**, *51* (2), 135–138. https://doi.org/10.1246/cl.210634.

(27) Si, Y.; Wang, W.; El-Sayed, E. S. M.; Yuan, D. Use of Breakthrough Experiment to Evaluate the Performance of Hydrogen Isotope Separation for Metal-Organic Frameworks M-MOF-74 (M=Co, Ni, Mg, Zn). *Sci China Chem* **2020**, *63* (7), 881–889. https://doi.org/10.1007/s11426-020-9722-2.

(28) el Osta, R.; Feyand, M.; Stock, N.; Millange, F.; Walton, R. I. Crystallisation Kinetics of Metal Organic Frameworks from in Situ Time-Resolved x-Ray Diffraction. In *Powder Diffraction*; 2013; Vol. 28, pp S256–S275. https://doi.org/10.1017/S0885715613000997.

(29) Luong, Q. T.; Choi, H. J.; Huynh, T. B. N.; Song, J.; Cho, Y.-H.; Kwon, O. J. Unraveling the Formation of Optimum Point in NiCo-Based Electrocatalysts for Urea Oxidation Reaction. *Electrochim Acta* **2022**, *431*, 141159. https://doi.org/10.1016/j.electacta.2022.141159.

(30) Vedharathinam, V.; Botte, G. G. Direct Evidence of the Mechanism for the Electro-Oxidation of Urea on Ni(OH)2 Catalyst in Alkaline Medium. *Electrochim Acta* **2013**, *108*, 660–665. https://doi.org/10.1016/j.electacta.2013.06.137.

(31) Putri, Y. M. T. A.; Jiwanti, P. K.; Irkham; Gunlazuardi, J.; Einaga, Y.; Ivandini, T. A. Nickel-Cobalt Modified Boron-Doped Diamond as an Electrode for Urea/H2O2 Fuel Cell. *Bull Chem Soc Jpn* **2021**, *94*, 2922–2928.

(32) Gamero-Quijano, A.; Huerta, F.; Salinas-Torres, D.; Morallón, E.; Montilla, F. Electrocatalytic Performance of SiO2-SWCNT Nanocomposites Prepared by Electroassisted Deposition. *Electrocatalysis* **2013**, *4* (4), 259–266. https://doi.org/10.1007/s12678-013-0144-3.

(33) Thakurathi, M.; Gurung, E.; Cetin, M. M.; Thalangamaarachchige, V. D.; Mayer, M. F.; Korzeniewski, C.; Quitevis, E. L. The Stokes-Einstein Equation and the Diffusion of Ferrocene in Imidazolium-Based Ionic Liquids Studied by Cyclic Voltammetry: Effects of Cation Ion Symmetry and Alkyl Chain Length. *Electrochim Acta* **2018**, *259*, 245–252. https://doi.org/10.1016/j.electacta.2017.10.149.

(34) Yang, D.; Yang, L.; Zhong, L.; Yu, X.; Feng, L. Urea Electro-Oxidation Efficiently Catalyzed by Nickel-Molybdenum Oxide Nanorods. *Electrochim Acta* **2019**, *295*, 524–531. https://doi.org/10.1016/j.electacta.2018.10.190.

(35) He, M.; Feng, C.; Liao, T.; Hu, S.; Wu, H.; Sun, Z. Low-Cost Ni2P/Ni0.96S Heterostructured Bifunctional Electrocatalyst toward Highly Efficient Overall Urea-Water Electrolysis. *ACS Appl Mater Interfaces* **2020**, *12* (2), 2225–2233. https://doi.org/10.1021/acsami.9b14350.

(36) Zhu, W.; Yue, Z.; Zhang, W.; Hu, N.; Luo, Z.; Ren, M.; Xu, Z.; Wei, Z.; Suo, Y.; Wang, J. Wet-Chemistry Topotactic Synthesis of Bimetallic Iron-Nickel Sulfide Nanoarrays: An Advanced and Versatile Catalyst for Energy Efficient Overall Water and Urea Electrolysis. *J Mater Chem A Mater* **2018**, *6* (10), 4346–4353. https://doi.org/10.1039/c7ta10584c.

(37) Chen, S.; Duan, J.; Vasileff, A.; Qiao, S. Z. Size Fractionation of Two-Dimensional Sub-Nanometer Thin Manganese Dioxide Crystals towards Superior Urea Electrocatalytic Conversion. *Angewandte Chemie* **2016**, *128* (11), 3868–3872. https://doi.org/10.1002/ange.201600387.

(38) Vedharathinam, V.; Botte, G. G. Understanding the Electro-Catalytic Oxidation Mechanism of Urea on Nickel Electrodes in Alkaline Medium. *Electrochim Acta* **2012**, *81*, 292–300. https://doi.org/10.1016/j.electacta.2012.07.007.

(39) Ye, K.; Zhang, D.; Guo, F.; Cheng, K.; Wang, G.; Cao, D. Highly Porous Nickel@carbon Sponge as a Novel Type of Three-Dimensional Anode with Low Cost for High Catalytic Performance of

Urea Electro-Oxidation in Alkaline Medium. *J Power Sources* **2015**, *283*, 408–415. https://doi.org/10.1016/j.jpowsour.2015.02.149.

Table of Content (ToC) Graphic